IRIS AperTO

UNIVERSITÀ DEGLI STUDI DI TORINO

AperTO - Archivio Istituzionale Open Access dell'Università di Torino

The (100), (110) and (111) surfaces of diamond: an ab initio B3LYP study

This is the author's manuscript

Original Citation:

Availability:

This version is available http://hdl.handle.net/2318/142785 since 2016-07-21T09:55:16Z

Published version:

DOI:10.1080/00268976.2013.829250

Terms of use:

Open Access

Anyone can freely access the full text of works made available as "Open Access". Works made available under a Creative Commons license can be used according to the terms and conditions of said license. Use of all other works requires consent of the right holder (author or publisher) if not exempted from copyright protection by the applicable law.

(Article begins on next page)

12 October 2024

This is the author's final version of the contribution published as:

DE LA PIERRE M.; BRUNO M.; MANFREDOTTI C.; NESTOLA F.; PRENCIPE M.; MANFREDOTTI C.. The (100), (110) and (111) surfaces of diamond: an ab initio B3LYP study. MOLECULAR PHYSICS. 112 pp: 1030-1039.
DOI: 10.1080/00268976.2013.829250

The publisher's version is available at:
http://www.tandfonline.com/doi/abs/10.1080/00268976.2013.829250

When citing, please refer to the published version.

Link to this full text:
http://hdl.handle.net/2318/142785

This full text was downloaded from iris - AperTO: https://iris.unito.it/

iris - AperTO

University of Turin's Institutional Research Information System and Open Access Institutional Repository

The (100), (111) and (110) surfaces of diamond: an *ab initio* B3LYP study

Marco DE LA PIERRE,[1,2] *Marco BRUNO,*[3] *Chiara MANFREDOTTI,*[2,4] *Fabrizio NESTOLA,*[5] *Mauro PRENCIPE,*[3] *Claudio MANFREDOTTI*[2,4]

[1]Dipartimento di Chimica, Università degli Studi di Torino, Via P. Giuria 7, Torino, I-10125

[2]NIS - Nanostructured Interfaces and Surfaces Centre of Excellence, Via P. Giuria 7, Torino, I-10125

[3]Dipartimento di Scienze della Terra, Università degli Studi di Torino, Via Valperga Caluso 35, Torino, I-10125.

[4]Dipartimento di Fisica, Università degli Studi di Torino, Via P. Giuria 1, Torino, I-10125

[5]Dipartimento di Geoscienze, Università di Padova, Via G. Gradenigo 6, Padova, I-35131

***Corresponding author**
Tel. +39 011 670 7560
Email: marco.delapierre@unito.it

Abstract

We present an accurate *ab initio* study of the structure and surface energy of the low-index (100), (111) and (110) diamond faces, by using the hybrid Hartree-Fock/Density Functional B3LYP Hamiltonian and a localized all-electron Gaussian-type basis set. A 2D periodic slab model has been adopted, for which convergence on both structural and energetic parameters has been thoroughly investigated. For all the three surfaces possible relaxations and reconstructions have been considered. A detailed geometrical characterization is provided for the most stable structure of each orientation; surface energy is discussed for all the investigated faces. All data show a very good agreement with previous pure Density Functional calculations.

Keywords Diamond, {100}, {111} and {110} forms, Surface structure, Surface reconstruction, Surface energy, Quantum-mechanical calculations, CRYSTAL code

1. Introduction

Diamonds and their inclusions (hereafter named Diamond Inclusions, DIs) are among the deepest materials originating from Earth's interior and reaching the planet surface. While being billions years old, they remain unaltered over time and preserve the pristine conditions of Earth. Therefore, their study plays a key role in understanding and interpreting the geodynamics, geophysics, petrology, geochemistry and mineralogy of the Earth's mantle from lithospheric to lower-mantle levels (Stachel and Harris [1], and references therein).

DIs reflect the chemical composition and mineral assemblages of the two principal rock types occurring in the deep lithosphere, namely peridotite and eclogite (e.g., [2]). Typical DIs of the peridotitic paragenesis are olivine, orthopyroxene, chromian diopsidic clinopyroxene, chromian pyropic garnet, magnesiochromite and iron–nickel sulfides, whereas typical eclogite minerals are omphacitic pyroxene, chromium-poor garnet, and iron-rich sulfides. DIs are divided into three groups (*protogenetic*, *syngenetic*, *epigenetic*), the criterion being whether their formation preceded, accompanied or followed crystallization of their host diamonds (e.g., [2]). DIs are classified as protogenetic when they formed before the encapsulation by the host diamond, whereas they are considered syngenetic when the inclusion and its host diamond formed at exactly the same time and by the same genetic process. Both groups play a key role in the study of diamond formation processes, contrary to epigenetic phases, that are secondary minerals, usually associated with crustal processes, and atypical to the primary minerals in mantle xenoliths.

Distinguishing between syngenesis and protogenesis is as crucial as extremely difficult and controversial, as demonstrated by Taylor et al. [3]. The most common observation used to deduce syngenesis is the imposition of the host diamond morphology on the DI (e.g., [2, 4-6]). However, as demonstrated by Taylor et al. [3], some peridotitic garnet inclusions, having morphology imposed by the host diamond, clearly show a Rare Earth Element (REE) pattern typical of garnets found worldwide and not included in diamonds. Taylor et al. [3] stated that this observation is consistent with a protogenetic nature, at least for peridotitic garnets. Similar conclusions were drawn by Thomassot et al. [7], who investigated isotopes of sulfide inclusions in diamonds, and Spetsius et al. [8], who analyzed inclusions found in zircons extracted from diamonds. These evidences suggest that at the moment no conclusive criteria exist, able to establish whether a diamond and inclusion pair is either syngenetic or protogenetic.

A significant contribution to this syngenesis/protogenesis debate is brought by the observation that some DIs occur in a specific orientation relationship with respect to diamond, which can be considered as a powerful proof in favor of epitaxial growth, and hence syngenesis [2, 5, 6, 9-15]. The first findings concerning possible epitaxial growth were those of Mitchell and Giardini [9], who reported oriented inclusions of olivine in diamonds: the orientation was such that the (010) face of olivine was parallel to the (111) one of the diamond and that the zone [101] of olivine was parallel to that [101] of diamond. More recent findings were reported by Wiggers de Vries et al. [16], whose electron backscatter diffraction experiments showed that the <100> crystallographic directions of diamond were parallel to the <100> directions of their chromite inclusions. These epitactic relationships seem to indicate an epitaxial growth of the DI above the diamond or viceversa.

A tool capable of interpreting the outlined experimental evidences and providing new insights in the diamond/DI interface system is quantum mechanical *ab initio* simulation. This

technique has the potential to investigate structure and stability of diamond/DI interfaces, as well as nucleation and growth mechanisms.

In the past, computer simulation has been applied to the study of the most typical growth planes of diamond, namely (100), (111) and (110), both in clean and hydrogen-terminated conditions. The main goal was to support and interpret the experimental findings concerning structure and reconstruction, energetics, electronic structure and chemical composition. The first applied methods include Modified Neglect of Differential Overlap [17], Tight Binding (TB) [18, 19], semi-empirical potentials [20, 21], Local Density Functional-Molecular Dynamics (LDF-MD) [22, 23]. The most systematic and extensive investigation was the one performed by Kern and coworkers [24-28], who adopted density functional theory (DFT) at the local density approximation (LDA) level, coupled with pseudo-potentials and plane waves to describe the wave-function. In subsequent works, the *ab initio* DFT approach was extended to the exploration of surface terminations other than hydrogen, such as oxygen and hydroxyl [29-32].

In the present study a hybrid Hartree-Fock (HF)-DFT approach has been adopted, which notably has never been applied before to the study of diamond surfaces. In particular, the chosen functional is B3LYP [33-35], which has already demonstrated great accuracy in describing the surfaces of insulating materials, such as periclase [36], silica [37-42], and hydroxyhapatite [43-48]. These works concerned the investigation of structure and energetics for variously oriented surfaces, as well as of their interactions with either simple probe molecules or organic compounds.

The first step for the investigation of diamond/DI interfaces is the assessment of our hybrid method in the description of clean diamond surfaces. Therefore, the present paper is devoted to the study of the structure and surface energy of the main growth forms of diamond, {100}, {111} and {110}, which are interested by epitaxial phenomena. The paper is structured as follows: (i) outline of the computational parameters used in the *ab initio* calculations of the (100), (111) and (110) surfaces of diamond; (ii) assessment of the slab model, i.e. determination of the minimum number of atomic layers required for convergence of the properties of interest; (iii) description of the structure and energy of the (100), (111) and (110) surfaces, and comparison with previous computational studies; (iv) main conclusions.

2. Computational details

The *ab initio* CRYSTAL09 code [49, 50] was employed, which implements the Hartree-Fock and Kohn-Sham self-consistent field (SCF) method for the study of periodic systems [51]. Surfaces were simulated by using the 2D periodic slab model, consisting of a film formed by a set of atomic layers parallel to the *hkl* crystalline plane of interest [52]. Selected outputs from the calculations are available as Supporting Information.

All the calculations were performed at the DFT (Density Functional Theory) level. In the Density Functional approach, the B3LYP Hamiltonian was adopted [33-35], which contains a hybrid Hartree-Fock/Density-Functional exchange term. This Hamiltonian has recently been successfully applied to the study of structural, vibrational and optical properties of carbon nanotubes and porous graphene phases [53-55].

The multi-electronic wave-function is constructed as an anti-symmetrized product (Slater determinant) of mono-electronic crystalline orbitals (COs) which are linear combinations of local

functions (i.e. atomic orbitals, AOs) centred on each atom of the crystal. In turn, AOs are linear combinations of Gaussian-type functions (GTF, the product of a Gaussian times a real solid spherical harmonic to give *s*-, *p*- and *d*-type AOs). In the present study, C was described with a 6-1111G* basis set [56], where the outer *sp* (0.175) and *d* (0.8625) coefficients were variationally optimized (the symbol * refers to the inclusion of *d* orbitals). The complete basis-set is available as Supporting Information. Additional calculations were performed with smaller 6-31G* and 6-211G* basis sets [56], to clarify the role of this relevant computational parameter in the calculation of the structural and energetic properties of diamond surfaces. Indeed, these basis sets yield comparable results with respect to the richer 6-1111G* basis set; a detailed comparison is included in the Supporting Information.

DFT Exchange and correlation contributions were evaluated numerically by integrating, over the cell volume, functions of the electron density and of its gradient. Choice of the integration grid is based on an atomic partition method, originally developed by Becke [57]. In the present study, the extra-large *pruned* (75, 974) *p* grid was chosen (XLGRID in the code, see Dovesi et al. [50]), which ensures a satisfactory accuracy in the integrated electron charge density, the corresponding error for the studied surfaces being smaller than $1\cdot10^{-4}$ |e| (over 144 |e|). The thresholds controlling the accuracy in the evaluation of Coulomb and exchange integrals (ITOL1, ITOL2, ITOL3, ITOL4 and ITOL5, see Dovesi et al. [50]) were set to 10^{-7} (ITOL1 to ITOL3), 10^{-8} (ITOL4) and 10^{-18} (ITOL5). Threshold on the SCF energy was set to 10^{-10} Ha. Diagonalization of the Hamiltonian for the studied surfaces was performed at 25 **k** points in the reciprocal space (Monkhrost net, see Monkhrost [58]) by setting the shrinking factor IS [50] to 8. Structures were optimized by using the analytical energy gradients with respect to atomic coordinates [59-61]; convergence was checked on both gradient components and nuclear displacements, whose tolerances where set to 0.0003 Hartree·bohr^{-1} and 0.0012 bohr, respectively.

The specific surface energy γ at T = 0 K was calculated by using the following relation [52]:

$$g = \lim_{n\to\infty} E_s(n) = \lim_{n\to\infty} \frac{E(n) - nE_{bulk}}{2A} \quad (1)$$

where *E(n)* is the energy of a *n*-layer slab; E_{bulk} is the energy of the bulk; *A* is the area of the primitive unit cell of the surface; the factor 2 in the denominator accounts for the upper and lower surfaces of the slab. $E_s(n)$ is thus the energy per unit area required for the formation of the surface from the bulk. As more layers are added in the calculation ($n \to \infty$), $E_s(n)$ will converge to the surface energy per unit area (γ). Values of the surface energy are reported both in J/m^2 and in eV/ surface atom (in the following, for brevity of notation we will use eV/atom). All values were corrected for Basis Set Superposition Error (BSSE, e.g. [38,52]).

Supplementary data to this article can be found online at -----

3. Results and discussion

3.1. Bulk parameters

A preliminary step of this study consisted in the calculation of the structural and energetic properties of bulk diamond. These data can be compared to experiment, permitting to evaluate the

accuracy of the adopted computational setup. Moreover, structural quantities will serve as reference for the subsequent analysis of diamond surfaces. Let us recall that bulk diamond has a $Fd\bar{3}m$ space group; its unit cell contains 2 atoms.

The fundamental structural parameter is the lattice parameter. Our B3LYP calculation yields a value of 3.5769 Å; the experimental datum is 3.567 Å [62], indicating only a slight (0.3%) overestimation. Derived quantities are the C-C bond distance of 1.5488 Å, and the inter-layer distances along the three crystallographic directions here investigated: 0.8942 Å along <100>, 0.5163 and 1.5488 Å along <111>, 1.2646 Å along <110>.

As regards energetics, the computed cohesive energy is 7.0427 eV/atom, to be compared with the experimental value of 7.62 eV/atom [63, 64]. Our method appears to underestimate this quantity by 7.6%.

3.2. Determination of the slab thickness to reproduce the (100), (110) and (111) surface properties

The key quantity that characterizes the slab model is the number of atomic layers composing the slab; here and in the following, atoms are considered to form a layer when they share the same z coordinate in the slab ideally cut from the bulk (i.e. whose geometry is still not optimized). The higher the number of layers, the more resembling to the bulk the slab properties will be; however, the computational cost will increase accordingly. It is then crucial to identify the minimum number of layers that is required to have good precision in describing the properties of interest. We were here interested in reproducing i) the specific surface energy; ii) the geometry of the surface (upper atomic layers) and eventually of the bulk (inner atomic layers); iii) the surface atomic net charges. We considered that properties are "well converged" when surface energy does not change within 0.01 eV/atom, distances within 0.01 Å, angles within 1°, charges within 0.01 |e|. Results for the three diamond surface orientations are shown in Table 1; notation for the examined quantities is defined in the caption to the Table 1. Note that for the (111) orientation both the 1x1 relaxed and 2x1 reconstructed structures were analyzed.

Let us consider the (100) surface (see Table 1). First of all, the surface energy γ is already quite stable with 8 layers (1.936 eV/atom), but reaches the desired convergence with 12 layers (1.945 eV/atom against 1.947 eV/atom for the 14-layer case). All bond angles θ and the atomic charge q(1) turn out to be stable for all the considered slab thicknesses; 8 layers are required for q(2). Concerning the bond lengths d, we notice that 6 layers are enough for describing the first two surface layers properly. In fact, in the case of d(1-1) and d(1-2) distances we have 1.3805 and 1.5238 Å when using 6 layers, to be compared with 1.3707, 1.5150 Å (14 layers). However, when inner atoms are considered, 8 layers are required: d(2-3*) and d(innest) are 1.5431, 1.4942 Å (6 layers), against 1.5718, 1.5438 Å (8 layers) and 1.5820, 1.5529 Å (14 layers); values of d(innest) can in turn be compared with the bulk value of 1.5488 Å. The reason for the slower convergence of the inner distances is surface reconstruction, which alters the surface structure with respect to the bulk one to a great extent; thus a higher number of layers is required to reach the ideal bulk geometry inside the slab. 10 layers are required when considering the inter-layer distance z. For example, z(1-2) and z(innest) are 0.6523, 0.7347 Å in a 8-layer slab, against 0.6781, 0.8927 Å (10 layers) and 0.6798, 0.8863 Å (14 layers); note the slightly large difference, 1.3 Å, for z(innest) with 12 layers (0.8736 Å vs. 0.8863 Å with 14 layers). When considering the intra-layer buckling of atoms Δz, occurring in the third and fourth layers, at least 12 layers are required, as in the case of

the 10-layer structure the differences are increasing for both quantities: Δz(3) and Δz(4) are 0.2787, 0.1782 Å (10 layers), to be compared with 0.2657, 0.1579 Å (12 layers) and 0.2646, 0.1560 Å (14 layers). Overall, inter-layer distances and intra-layer buckling are the slowest converging properties; surface reconstruction here probably plays a cumulative effect, as a large number of atoms and bonds is involved in determining the equilibrium distance between two atomic layers.

The case of the (111) surface is the most delicate. When dealing with the 1x1 relaxed structure, SCF issues were encountered during the electronic structure calculations. The reason lies in the electronic surface states of this unsaturated, conducting structure, that are delocalized all over the diamond surface; when few atomic layers are considered, the high relative weight of these states in the band structure destabilizes the calculation and hinders to reach convergence in the SCF calculation of the total energy. As a consequence, in this case at least 10 layers are required to successfully optimize the structure. When considering the structures with 10, 12 and 14 layers (see Table 1), we notice that convergence for all the observed quantities is already reached in the 10-layer case. This is reasonable, as no reconstruction occurs for this surface, so that there are no huge geometrical rearrangements.

Let us now consider the (111)-2x1 reconstructed structure. Here at least 8 layers are required to permit the realization of the large and in-deep reconstruction. Moreover, given the peculiar geometry of this structure, only a number of layers which is multiple of 4 is permitted: the cases of 8, 12 and 16 layers were considered. The surface energy values are 1.364 (8 layers), 1.307 (12 layers) and 1.304 (16 layers) eV/atom; thus, this quantity is converged with 12 layers. The four surface-layer distances reported in the Table 1 are already converged with 8 layers, as well as the first-layer angle θ(1*) and the second-layer angle θ(2c). All other quantities require 12 layers for convergence. In particular, for the distance d(innest) compare 1.4678 Å (8 layers) with 1.5380 Å (12 layers), 1.5419 Å (16 layers) and 1.5488 (bulk structure); due to the huge reconstruction, the value at 16 layers still differs from the bulk one by 0.69 Å. Note that, in the case of the intra-layer buckling Δz(5), only two values are available, with 12 (0.0558 Å) and 16 (0.0666 Å) layers, whose difference is 0.01 Å; we can consider this quantity to be converged, given the good trends observed for the other distances in this structure.

Finally, the case of (110) surface is quite simple to analyze. Similar to the case of the (111)-1x1 relaxed structure, no surface reconstruction takes place; all the quantities under study reach convergence when the 6-layer slab is considered, except for the surface energy and the inter-layer distance z(innest), which require 8 layers.

To sum up the results of this section, (100) and (111)-2x1 faces require at least 12 layers to be described with the desired precision. 10 layers are necessary for the (111)-1x1 face. In the case of the (110) face, 8 layers are enough. However, in the following discussion data for all surfaces refer to the case with 12 layers, to use the maximum precision available in this study with a homogeneous number of layers.

3.3. Structure and surface energy of the (100) surface

The ideal structure of the (100) surface presents atoms with two dangling bonds (see Figure S1, Supporting Information). Such a condition is strongly unfavourable from an energetic point of view, and the surface undergoes a 2x1 reconstruction. A graphical representation is given in Figure 1, whereas the structural parameters are reported in Table 2, along with data taken from the literature.

The surface unit cell is doubled with respect to the bulk one. This condition allows the formation of surface C-C dimers, so that each surface atom partially saturates its dangling bonds, thus lowering the total energy. This is reflected in the changes in the surface geometry: the C-C distance in the dimer is 1.371 Å, far lower than the value for bulk diamond (1.549 Å, sp^3 C), a little bit lower than in graphite (1.42 Å, sp^2 C), and almost equal to the case of ethylene molecule (1.38 Å, again sp^2 C). Bond angles of surface carbons are 108.6° and 113.2°, not far from the value of a tetrahedral coordination (109.5°), but indeed quite far from the one of a planar sp^2-like coordination (120°). On the basis of these structural parameters, we can state that surface dimers show a double bond together with a distorted, unsaturated, sp^3-like coordination. As a consequence of the three-fold coordination, surface atoms feature stronger bonds with atoms of the second layer, too: this is confirmed by the d(1-2) distances (1.515 Å), and most of all by the inter-layer distance, which is 0.678 Å, 0.217 Å lower than the value for bulk diamond. The 2x1 reconstruction also implies the occurrence of two not equivalent carbon sites, which results in the buckling of the atoms belonging to the sub-surface layers: atoms are displaced along the z axis by 0.266 and 0.158 Å in the third and fourth layers, respectively. Buckling of the first layer dimers was checked by calculation and was found to be energetically unfavourable.

When comparing the obtained geometry with previous published data, the results are qualitatively the same in all cases (Table 2). With respect to the *ab initio* pure DFT studies by Fürthmuller et al. [27], Hong and Chou [65] and Steckel et al. [66], the values are the same within 0.01 Å, which is pretty satisfactory. Instead, molecular dynamics studies performed by Alfonso et al. [23] and Davisdon and Pickett [19] show larger discrepancies; however, in these cases the theoretical framework is known to be less accurate than our *ab initio* approach.

Surface energy values for all the investigated diamond faces are summarized in Table 3. In the case of the (100) face, the 1x1 ideal (not relaxed) and 1x1 relaxed surface energies are 3.742 eV/atom (9.372 J/m^2) and 3.642 eV/atom (9.122 J/m^2), respectively; relaxation accounts for -0.100 eV/atom. As expected, the (100)-2x1 reconstructed surface shows the lowest surface energy, 1.945 eV/atom (4.870 J/m^2). As a matter of fact, the 2x1 reconstruction results in an energy gain equal to -1.797 eV/atom with respect to the ideal surface, which is a significant stabilization. The main factor for the surface stabilization is the formation of the strongly bonded C-C dimers; on the other hand, a small, minor destabilization effect is probably associated to the geometry distortion of the first two atomic layers. When comparing to literature, Kern and Hafner [28] reported values of -0.26 and -1.77 eV/atom, for the relaxation and reconstruction energies, respectively; Steckel et al. [66] found -0.12 and -1.58 eV/atom for the same quantities. Finally, a reconstruction energy of -1.86 eV/atom was estimated by Davidson and Pickett [19] (molecular dynamics). Thus, while the predicted relative stability is always the same, quantitative results are spread over a 10 % range of values.

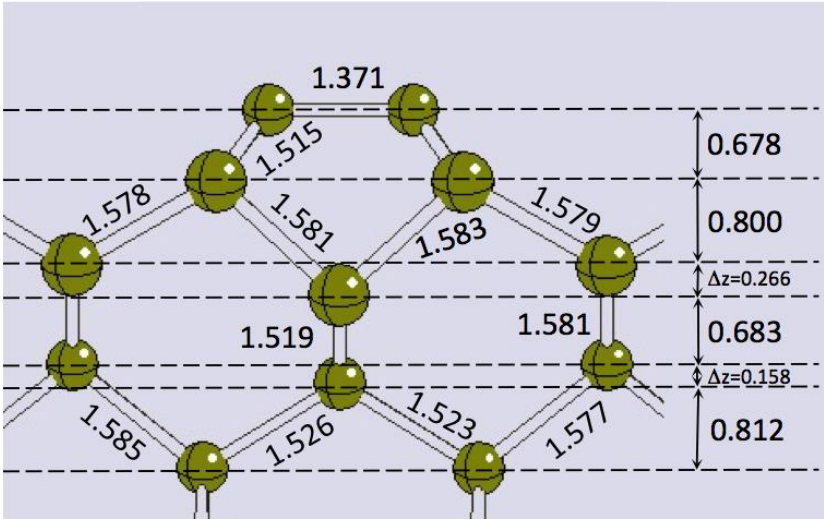

Figure 1. Section of the (100)-2x1 reconstructed diamond surface. All values are in Å; Δz is the intra-layer buckling.

3.4. Structure and surface energy of the (111) surface

The (111) surface can have two different terminations (see Figures S3 and S4, Supporting Information). Surface carbon atoms feature one and three dangling bonds in the two cases, respectively. As the former condition is by far the most stable, our structural investigations concentrated on this configuration. The (111) surface with one dangling bond per surface atoms undergoes a strong 2x1 reconstruction, called Pandey-chain reconstruction [67]. The corresponding optimized structure is shown in Figure 2; structural parameters are given in Table 2. The first two surface layers are affected to a large extent: the section view clearly shows an alternation of 5-atoms and 7-atoms rings, contrary to all other diamond structures, where the 6-atoms ring is always found. The main consequence of the reconstruction is the formation of "zig-zag" chains of C atoms at the surface, featuring a geometry very close to that of graphite: the C-C distance is 1.443 Å, while the bond angle is 122.4° (graphite features 1.42 Å and 120°). This configuration allows for the formation of a delocalized π-bond along the surface atoms, which stabilizes the surface. The arrangement of the lower-lying atoms is a consequence of the constraints imposed by the "zig-zag" chains, and is quite peculiar: considering the first four atomic layers, bond distances range from 1.443 to 1.646 Å, while bond angles from 96.3° to 124.7°. Inter-layer distances are far from the bulk values in the case of the first two layers: z(1-2) and z(2-3) are equal to 0.694 and 1.511 Å, respectively (against 0.516 and 1.549 Å in the bulk). Finally, a remarkable intra-layer buckling is found in the case of the fourth and fifth layers: 0.177 and 0.056 Å, respectively. Both buckling and dimerization of the carbon atoms involved in the "zig-zag" chain was checked: they were found to be energetically unfavourable. Note that a 12-layer slab model is the smallest one that is suitable to properly describe the structural rearrangement in the (111)-2x1 reconstructed surface. A good agreement with literature can be found (Table 2); a slight overestimation of the bond distances is noticed, in particular in the case of d(1-2) and d(2-3) distances.

The relative stability of different (111) surfaces can be discussed by looking at Table 3. The surface with three dangling bond per C atom, 1x1-3db, either ideal or relaxed, is by far the least stable: the surface energy is 4.516 (13.060) and 4.501 (13.017) eV/atom (J/m^2), respectively. Let us

discuss the surface with one dangling bond per C atom. The ideal (not relaxed) 1x1 face presents a surface energy of 2.809 eV/atom (8.123 J/m^2); the relaxation of this surface corresponds to an energy gain of -0.567 eV/atom. However, the Pandey-chain reconstruction implies a far larger stabilization, equal to -1.502 and -0.935 eV/atom, with respect to the ideal and relaxed 1x1 surface, respectively. This stabilization is due to the formation of the π-bonded chain, which permits to saturate the fourth dangling bond of the surface C atoms; the relaxed 1x1 geometry is not suitable for this purpose. The comparison with other *ab initio* studies is satisfactory, in particular with the systematic work by Kern et Hafner [28], where the relaxation energy was estimated as 0.57 eV/atom and the reconstruction energies as -1.40 and -0.83 eV/atom, with differences below 10%. On the other hand, molecular dynamics calculations turn out to be less precise, as already pointed out before.

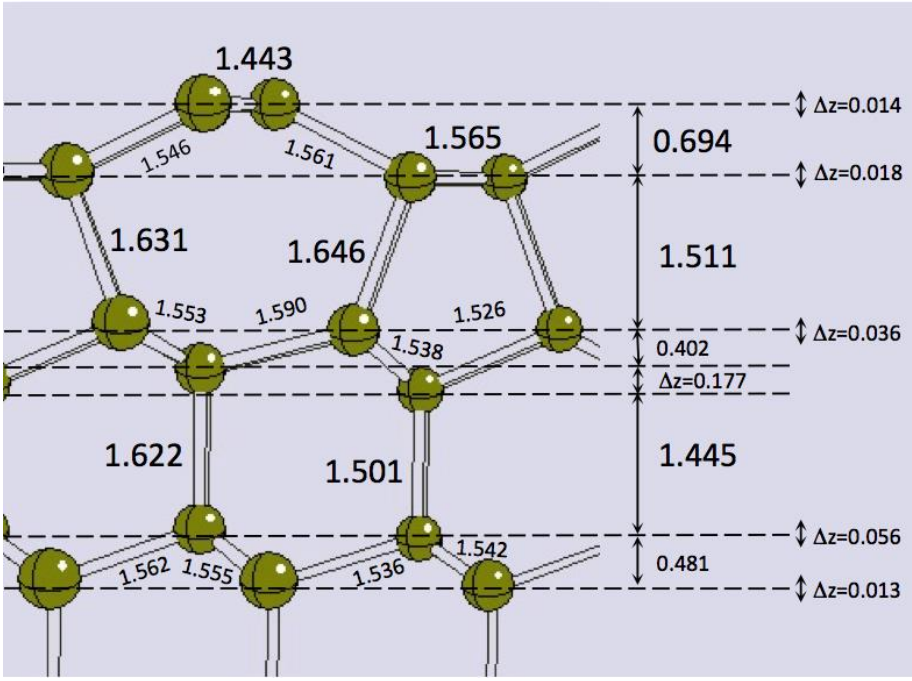

Figure 2. Section of the (111)-2x1 reconstructed diamond surface. All values are in Å; Δz is the intra-layer buckling.

3.5. Structure and surface energy of the (110) surface

The (110) surface does not undergo any reconstruction (see Figure 3 and Table 2). A simple relaxation of the first two atomic layers is sufficient to create a π-bonded "zig-zag" chain over the surface, with distances and angles very close to the values of both (111)-2x1 diamond surfaces and graphite: 1.434 Å and 123.7°, respectively. Similar to the case of the (111)-2x1 reconstructed surface, this configuration saturates the fourth dangling bond of surface carbons, with a stabilization effect. d(1-2) bond length is 1.480 Å, while z(1-2) and z(1-3) are 1.057 and 1.302 Å, respectively (the bulk value is 1.265 Å). From the third layer on, the bulk geometry is almost completely recovered. As for previous surfaces, quantitative agreement is found with the DFT study by Kern and Hafner [28]. Structures featuring either dimerization or buckling of the surface layer turn out to

be unstable with respect to the described surface; this is in agreement with previous *ab initio* results by Kern and Hafner [28], and in contrast with the molecular dynamics study by Alfonso et al. [23].

Concerning surface energy of the (110) face (see Table 3), we obtained 2.113 eV/atom (7.482 J/m^2) and 1.571 eV/atom (6.524 J/m^2) for the ideal and relaxed surfaces, respectively; the relaxation of the clean surface accounts for -0.542 eV/atom. As in the case of previous surfaces, the agreement turns out to be very satisfactory when referring to *ab initio* pure DFT studies [28], whereas surface energy values coming from molecular dynamics calculations [19] are very imprecise.

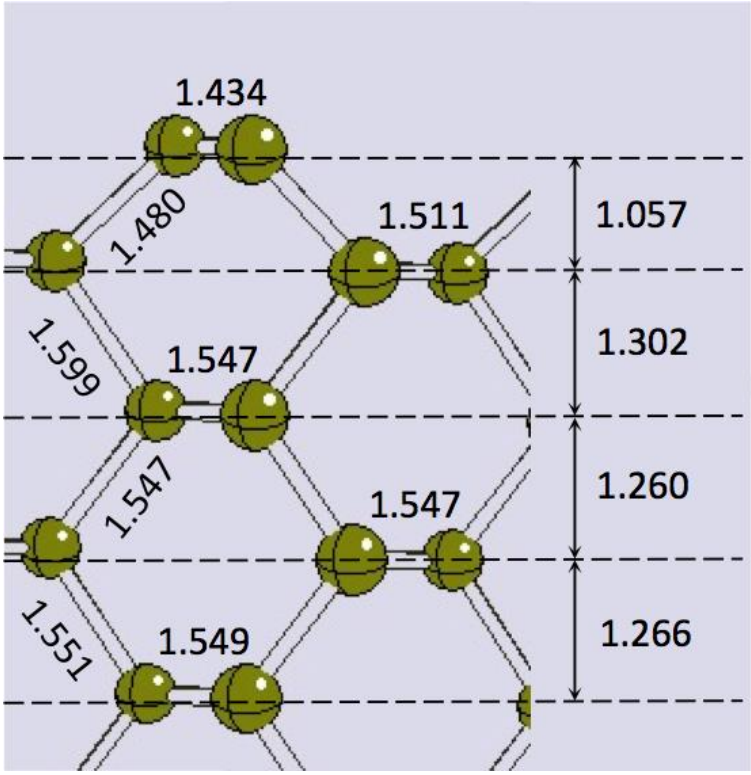

Figure 3. Section of the (110)-1x1 relaxed diamond surface. All values are in Å.

4. Conclusions

In this work, we have presented an accurate *ab initio* study of the structure and surface energy of the low-index (100), (111) and (110) diamond faces, by using for the first time, at the best of our knowledge, the hybrid Hartree-Fock/Density Functional B3LYP Hamiltonian and a localized all-electron Gaussian-type basis set. We can summarize our results in the following points:

(i) In order to reproduce the structure and surface energy of the studied diamond faces with satisfactory precision, the following slab thicknesses must be considered: the (100) and (111)-2x1 faces require at least 12 layers; 10 layers are necessary for the (111)-1x1 face; instead, instead, 8 layers are enough for the (110) face.

(ii) The (100) surface undergoes a 2x1 reconstruction. This condition allows the formation of surface C-C dimers, so that each surface atom partially saturates its dangling bonds, thus lowering the total energy. Indeed, the (100)-2x1 reconstructed surface shows a lower surface energy, 1.945 eV/atom (4.870 J/m^2), with respect to the relaxed (100)-1x1 surface, 3.642 (9.122) eV/atom (J/m^2).

(iii) As for the (100) face, also the (111) face is stabilized by a 2x1 reconstruction, called Pandey-chain reconstruction [67]. The main consequence of this reconstruction is the formation of π-bonded "zig-zag" chains of C atoms at the surface, whose geometrical parameters are very close to those of graphite. The surface energy of the (111)-2x1 face is 1.307 (3.780) eV/atom (J/m^2), whereas that of the relaxed (111)-1x1 surface is somewhat higher, 2.242 (6.483) eV/atom (J/m^2).

(iv) The (110) surface does not undergo any reconstruction. A relaxation of the first two atomic layers is sufficient to create π-bonded "zig-zag" chains over the surface, with a geometry very close to the values of both (111)-2x1 diamond surfaces and graphite. The surface energy is 1.571 (6.524) eV/atom (J/m^2).

(v) As a final remark on surface energies (in J/m^2), when considering the most stable structure for each crystallographic orientation, the relative stability we obtain is the same than for the LDA studies by Kern and Hafner [28] and Hong and Chou [68], despite the large percentage discrepancies: (111) < (100) < (110).

This paper is the first one of a series dedicated to the study of diamond by means of the B3LYP Hamiltonian. Indeed, future works will be devoted to the study of the interfaces between diamond/olivine and diamond/garnet and of functionalized diamond surfaces. Therefore, the calculations presented in this paper have permitted both i) to assess the performance of the B3LYP Hamiltonian in reproducing the structure and surface energy of the principal diamond faces and ii) to calibrate the computational parameters for future studies.

Acknowledgements

M. De La Pierre acknowledges Compagnia di San Paolo for financial support (Progetti di Ricerca di Ateneo-Compagnia di San Paolo-2011-Linea 1A, progetto ORTO11RRT5). F. Nestola and M. Bruno were supported by ERC Starting Grant 2012 (grant agreement n° 307322).

References

[1] T. Stachel, J.W. Harris, Ore Geol. Rev. 34 (2008) 5.
[2] H.O.A. Meyer, in: Mantle Xenoliths, Ed. P.H. Nixon (John Wiley & Sons, Chichester, 1987) p. 844.
[3] L.A. Taylor, M. Anand, P. Promprated, Proceedings of the 8th International Kimberlite Conference, 1 (2003) 1.
[4] J.W. Harris, Ind. Diam. Rev. 28 (1968) 402.
[5] H.O.A. Meyer, Am. Min. 70 (1985) 344.

[6] D.G. Pearson, S.B. Shirey, in: Application of Radiogenic Isotopes to Ore Deposit Research and Exploration. Reviews in Economic Geology, Vol. 12, Eds. D.D. Lambert and J. Ruiz (Society of Economic Geologists, Littleton CO, Denver, 1999) p. 199.
[7] E. Thomassot, P. Cartigny, J.W. Harris, J.P. Lorand, C. Rollion-Bard, M. Chaussidon, Earth Planet. Sci. Lett. 282 (2009) 79.
[8] Z.V. Spetsius, E.A. Belousova, W.L. Griffin, Suzanne Y. O'Reilly, N.J. Pearson, Earth Planet. Sci. Lett. 199 (2002) 111.
[9] R.S. Mitchell, A.A. Giardini, Am. Miner. 38 (1953) 136.
[10] S.I. Futergendler, V.A. Frank-Kamenetsky, Zapiski Vsesoyuznogo Mineralogicheskogo Obshestva 90 (1961) 230 (in Russian).
[11] J.L. Orlov, The mineralogy of diamond (Wiley, New York, 1977).
[12] N.V. Sobolev, Deep-seated inclusions in kimberlites and the problem of the composition of the upper mantle (American Geophysical Union, Washington, DC, 1977).
[13] J.W. Harris, J.J. Gurney, in: The properties of diamond, Ed. J.E. Field (Academic Press, London, 1979) p. 674.
[14] O. Leeder, R. Thomas, W. Klemm, Einschlusse in Mineralien (VEB Deutscher Verlag fur Grunstoffenindustrie, Leipzig, 1987).
[15] G.P. Bulanova, J.Geochem. Explor. 53 (1995) 1.
[16] D.F. Wiggers de Vries, M.R. Drury, D.A.M. de Winter, G.P. Bulanova, D.G. Pearson, G.R. Davies, Contrib. Mineral. Petrol. 161 (2011) 565.
[17] W.S. Verwoerd, Surf. Sci. 108 (1981) 153.
[18] F. Bechstedt, D. Reichardt, Surf. Sci. 202 (1988) 83.
[19] B.N. Davidson, W.E. Pickett, Phys. Rev. B 49 (1994) 11253.
[20] D.W. Brenner, Phys. Rev. B 42 (1990) 9458.
[21] J.A. Harrison, C.T. White, R.J. Colton, D.W. Brenner, Mater. Res. Soc. Bull. 18 (1993) 50.
[22] S. Iarlori, G. Galli, P. Gygi, M. Parinello, E. Tosatti, Phys. Rev. Lett. 69 (1992) 2947.
[23] D.R. Alfonso, D.A. Drabold, S.E. Ulloa, Phys. Rev. B 51 (1995) 14669.
[24] G.Kern, J. Hafner, J. Furthmüller, G. Kresse, Surf. Sci. 352-354 (1996) 745.
[25] G.Kern, J. Hafner, G. Kresse, Surf. Sci. 366 (1996) 445.
[26] G.Kern, J. Hafner, G. Kresse, Surf. Sci. 366 (1996) 464.
[27] J. Furthmüller, J. Hafner, G. Kresse, Phys. Rev. B 53 (1996) 7334.
[28] G. Kern, J. Hafner, Phys. Rev. B 56 (1997) 4203.
[29] S.J. Sque, R. Jones, P.R. Briddon, Phys. Rev. B 73 (2006) 085313.
[30] D. Petrini, K. Larsson, J. Phys. Chem. C 111 (2007) 795.
[31] D. Petrini, K. Larsson, J. Phys. Chem. C 112 (2008) 3018.
[32] G. Zilibotti, M.C. Righi, M. Ferrario, Phys. Rev. B 79 (2009) 075420.
[33] A. D. Becke, J. Chem. Phys. 98 (1993) 5648.
[34] C. Lee, W. Yang, R.G. Parr, Phys. Rev. B 37 (1988) 785.
[35] P.J. Stephens, F.J. Devlin, C.F. Chabalowski, M.J. Frisch, J. Phys. Chem. 98 (1994) 11623.
[36] A. Damin, R. Doves, A. Zecchina, P. Ugliengo, Surf. Sci. 479 (2001) 255.
[37] B. Civalleri, S. Casassa, E. Garrone, C. Pisani, P. Ugliengo, J. Phys. Chem. B 103 (1999) 2165.
[38] B. Civalleri, P. Ugliengo, J. Phys. Chem. B 104 (2000) 9491.
[39] A. Rimola, M. Sodupe, S. Tosoni, B. Civalleri, P. Ugliengo, Langmuir 22 (2006) 6593.
[40] A. Rimola, B. Civalleri, P. Ugliengo, Langmuir 24 (2008) 14027.

[41] S. Tosoni, B. Civalleri, P. Ugliengo, J. Phys. Chem. C 114 (2010) 19984.
[42] F. Musso, P. Ugliengo, M. Sodupe, J. Phys. Chem. A 115 (2011) 11221.
[43] M. Corno, A. Rimola, V. Bolis, P. Ugliengo, Phys. Chem. Chem. Phys. 12 (2010) 6309.
[44] P. Canepa, F. Chiatti, M. Corno, Y. Sakhno, G. Martra, P. Ugliengo, Phys. Chem. Chem. Phys. 13 (2011) 1099.
[45] A. Rimola, Y. Sakhno, L. Bertinetti, M. Lelli, G. Martra, P. Ugliengo, J. Phys. Chem. Lett. 2 (2011) 1390.
[46] A. Rimola, M. Aschi, R. Orlando, P. Ugliengo, J. Am. Chem. Soc. 134 (2012) 10899.
[47] F. Chiatti, M. Corno, P. Ugliengo, J. Phys. Chem. C 116 (2012) 6108.
[48] E. Jimenez-Izal, F. Chiatti, M. Corno, A. Rimola, P. Ugliengo, J. Phys. Chem. C 116 (2012) 14561.
[49] R. Dovesi, R. Orlando, B. Civalleri, C. Roetti, V.R. Saunders, C.M. Zicovich-Wilson, Z. Kristallogr. 220 (2005) 571.
[50] R. Dovesi et al., CRYSTAL09 User's Manual (University of Torino, Torino, Italy, 2009).
[51] C. Pisani, R. Dovesi, C. Roetti, Hartree-Fock ab-initio treatment of crystalline systems, Lecture Notes in Chemistry (Springer, Berlin, Heidelberg, New York, 1988).
[52] R. Dovesi, B. Civalleri, R. Orlando, C. Roetti, V. R. Saunders, in: Reviews in Computational Chemistry, Vol. 21, Eds. B. K. Lipkowitz, R. Larter and T. R. Cundari (John Wiley & Sons, Inc, New York, 2005) p. 443.
[53] Y. Noël, Ph. D'Arco, R. Demichelis, C.M. Zicovich-Wilson, R. Dovesi, J. Comput. Chem. 31 (2010) 855.
[54] R. Demichelis, Y. Noël, Ph. D'Arco, M. Rérat, C.M. Zicovich-Wilson, R. Dovesi, J. Phys. Chem. C 115 (2011) 8876.
[55] M. De La Pierre, P. Karamanis, J. Baima, R. Orlando, C. Pouchan, R. Dovesi, J. Phys. Chem. C 117 (2013) 2222.
[56] L. Ge, B. Montanari, J.H. Jefferson, D.G. Pettifor, N.M. Harrison, G.A.D. Briggs, Phys. Rev. B 77 (2008) 235416.
[57] A.D. Becke, Phys. Rev. A 38 (1988) 3098.
[58] H. J. Monkhrost, J. D. Pack, Phys. Rev. B 8 (1976) 5188.
[59] B. Civalleri, Ph. D'Arco, R. Orlando, V.R. Saunders, R. Dovesi, Chem. Phys. Lett. 348 (2001) 131.
[60] K. Doll, Comp. Phys. Commun. 137 (2001) 74.
[61] K. Doll, V.R. Saunders, N.M. Harrison, Int. J. Quantum. Chem. 82 (2001) 1.
[62] S.M. Sze, Semiconductor Devices: Physics and Technology (John Wiley and Sons Inc., New York, 2001).
[63] H.D. Hagstrum, Phys. Rev. 72 (1947) 947.
[64] A. Zunger, A.J. Freeman, Phys. Rev. B 15 (1977) 5049.
[65] S. Hong, M.Y. Chou, Phys. Rev. B 55 (1997) 9975.
[66] J.A. Steckel, G. Kresse, J. Hafner, Phys. Rev. B 66 (2002) 155406.
[67] K.C. Pandey, Phys. Rev. B 25 (1982) 4338.
[68] S. Hong, M.Y. Chou, Phys. Rev. B 57 (1998) 6262.

Tables

Table 1. Convergence of the surface energy γ and of selected structural parameters of diamond surfaces with respect to the number of layers of the slab model. Studied cases are: (100)-2x1 reconstructed, (111)-1x1 relaxed, (111)-2x1 reconstructed, and (110)-1x1 relaxed. Distances are in Å; angles are in degrees (°). γ is the surface energy at T = 0 K, in eV/surface atom. d(i-j) are bond distances between pairs of atoms lying in the ith and j^{th} layer (numbering begins from the surface layer); θ(i) are bond angles centered on atoms lying in the ith layer; *z*(i-j) are distances between pairs of atomic layers i and j; Δz(i) is the buckling of the ith layer, i.e. the displacement along the *z* axis of atoms within the same layer; q(i) is the net electronic charge of atoms lying in the ith layer. Notes: d(2-3*) and θ(2*) in (100) refer to the atoms underlying the surface "dimer"; θ(1*) in (110) and (111) is the angle among atoms belonging to the "zig-zag" surface chain.

	n. of layers	6	8	10	12	14	16
(100)-2x1	γ	2.175	1.936	1.923	1.945	1.947	
	d(1-1)	1.3805	1.3705	1.3698	1.3706	1.3707	
	d(1-2)	1.5238	1.5148	1.5143	1.5150	1.5150	
	d(2-3*)	1.5431	1.5718	1.5863	1.5813	1.5820	
	d(innest)	1.4942	1.5438	1.5479	1.5485	1.5529	
	θ(1a)	108.56	108.50	108.63	108.61	108.61	
	θ(1b)	112.18	113.26	113.26	113.19	113.18	
	θ(2*)	93.13	94.16	93.87	93.84	93.82	
	z(1-2)	0.6981	0.6523	0.6781	0.6777	0.6798	
	z(2-3)	0.8914	0.7823	0.7940	0.7996	0.8014	
	z(innest)	0.7958	0.7347	0.8927	0.8736	0.8863	
	Δz(3)	0.1087	0.2714	0.2787	0.2657	0.2646	
	Δz(4)	--	0.1672	0.1782	0.1579	0.1560	
	q(1)	5.855	5.847	5.842	5.841	5.842	
	q(2)	6.049	6.080	6.073	6.070	6.071	
(111)-1x1	γ	--	--	2.243	2.242	2.242	
	d(1-2)	--	--	1.4845	1.4844	1.4844	
	d(2-3)	--	--	1.6965	1.6976	1.6979	
	d(innest)	--	--	1.5473	1.5516	1.5485	
	θ(1)	--	--	116.84	116.84	116.84	
	θ(2)	--	--	100.37	100.36	100.35	
	z(1-2)	--	--	0.2671	0.2668	0.2668	
	z(2-3)	--	--	1.6965	1.6976	1.6979	
	z(innest)	--	--	0.5117	0.5132	0.5154	
	q(1)	--	--	5.761	5.760	5.760	
	q(2)	--	--	6.226	6.227	6.227	
(111)-2x1	γ	--	1.364	--	1.307	--	1.304
	d(1-1)	--	1.4428	--	1.4430	--	1.4431
	d(1-2)a	--	1.5485	--	1.5463	--	1.5448
	d(1-2)b	--	1.5545	--	1.5611	--	1.5617
	d(2-2)	--	1.5680	--	1.5653	--	1.5648
	d(innest)	--	1.4678	--	1.5380	--	1.5419
	θ(1*)	--	122.45	--	122.42	--	122.40
	θ(2a)	--	97.54	--	96.33	--	95.99
	θ(2b)	--	96.52	--	97.64	--	97.82
	θ(2c)	--	107.52	--	107.78	--	107.84
	z(1-2)	--	0.7054	--	0.6942	--	0.6896

	z(2-3)	--	1.5354	--	1.5107	--	1.5081
	z(innest)	--	1.4678	--	1.5380	--	1.5419
	Δz(4)	--	0.1231	--	0.1769	--	0.1813
	Δz(5)	--	--	--	0.0558	--	0.0666
	q(1)	--	5.911	--	5.886	--	5.880
	q(2)	--	6.065	--	6.061	--	6.060
(110)-1x1	γ	1.546	1.565	1.570	1.571	1.572	
	d(1-1)	1.4342	1.4344	1.4344	1.4344	1.4344	
	d(1-2)	1.4790	1.4801	1.4803	1.4803	1.4803	
	d(2-2)	1.5095	1.5109	1.5112	1.5112	1.5112	
	d(innest)	1.5442	1.5535	1.5486	1.5489	1.5485	
	θ(1*)	123.71	123.68	123.68	123.67	123.67	
	θ(2a)	99.84	100.00	100.03	100.04	100.04	
	θ(2b)	113.82	113.65	113.62	113.61	113.61	
	z(1-2)	1.0535	1.0565	1.0570	1.0570	1.0571	
	z(2-3)	1.3042	1.3018	1.3016	1.3016	1.3016	
	z(innest)	1.2534	1.2680	1.2637	1.2645	1.2642	
	q(1)	5.898	5.898	5.899	5.899	5.899	
	q(2)	6.096	6.098	6.096	6.096	6.096	

Table 2. Structural parameters of the most stable (100), (111) and (110) diamond surfaces. Lengths are in Å; angles are in degrees (°). d(i-j) are bond distances between pairs of atoms lying in the ith and j^{th} layer (numbering begins from the surface layer); *z*(i-j) are distances between pairs of atomic layers i and j; Δz(i) is the buckling of the ith layer; in the case of (110) surface, z(i) is the layer relaxation along the z coordinate with respect to the ideal surface.

(100)-2x1								
	This work	Steckel (GGA)[a]	Furthmuller (LDA)[b]	Hong (LDA)[c]	Alfonso (LDA-MD)[d]	Davidson (TB-MD)[e]	Sque (LDA)[f]	Petrini (GGA)[g]
d(1-1)	1.371	1.38	1.37	1.37	1.36	1.4	1.37	1.381
d(1-2)	1.515	1.51	1.50	1.50			1.50	1.563
z(1-2)	0.678		0.67		0.68	0.67	0.68	
z(2-3)	0.800		0.79				0.79	
Δz(3)	0.266		0.26		0.13		0.26	
Δz(4)	0.158		0.16		0.25		0.15	

(111)-2x1						
	This work	Kern (LDA)[h]	Alfonso (LDA-MD)[d]	Davidson (TB-MD)[e]	Sque (LDA)[f]	Petrini (GGA)[i]
d(1-1)	1.443	1.43	1.44	1.44	1.43	1.44
d(1-2)	1.546	1.53		1.47	1.53	1.54
	1.561					
d(2-2)	1.565	1.54	1.56		1.54	1.56
d(2-3)	1.631	1.60			1.60	1.62
	1.646	1.63		1.69	1.63	
z(1-2)	0.694				0.69	
z(2-3)	1.511				1.52	
Δz(4)	0.177	0.17			0.18	
Δz(5)	0.056	0.06			0.07	

(110)-1x1				
	This work	Kern (LDA)[j]	Alfonso (LDA-MD)[d]	Davidson (TB-MD)[e]
d(1-1)	1.434	1.419	1.44	1.43
d(1-2)	1.480	1.467		
z(1-2)	1.057			1.08
z(2-3)	1.302			1.30
z(1)	-0.175	-0.17		
z(2)	0.033	0.03		
Δz(1)	0.000	0.00	0.14	0.00

[a]Steckel et al. [66]; [b]Furthmüller et al. [27]; [c]Hong and Chou [65]; [d]Alfonso et al. [23]; [e]Davidson and Pickett [19]; [f]Sque et al. [29]; [g]Petrini and Larsson [30]; [h]Kern et al. [25, 26]; [i]Petrini and Larsson [31]; [j]Kern and Hafner [28].

Table 3. Surface energy γ at T = 0 K of the (100), (111) and (110) surfaces of diamonds. Values are in eV/surface atom; bracketed values are in J/m^2. In the case of energy differences, the reference structure is marked with a hash "#".

	This work	Kern (LDA)[a]	Steckel (GGA)[b]	Alfonso (LDA-MD)[c]	Davidson (TB-MD)[d]	Sque (LDA)[e]	Hong (LDA)[f]
			(100)				
1x1 ideal	3.742 (9.372)	3.89	3.48		#		
1x1 relaxed	3.642 (9.122)	3.63	3.36				
2x1 reconstructed	1.945 (4.870)	2.12	1.90		# -1.86		(5.60)
			(111)				
1x1-3db ideal	4.516 (13.060)	4.65					
1x1-3db relaxed	4.501 (13.017)	4.63					
1x1 ideal	2.809 (8.123)	2.75			#		
1x1 relaxed	2.242 (6.483)	2.18		#	# -0.39	#	
2x1 reconstructed	1.307 (3.780)	1.35		# -0.63	# -1.08	# -0.80	(4.12)
			(110)				
1x1 ideal	2.113 (7.482)	2.09			#		
1x1 relaxed	1.571 (6.524)	1.66			# -0.38		(5.96)

[a]Kern and Hafner [28]; [b]Steckel et al. [66]; [c]Alfonso et al. [23]; [d]Davidson and Pickett [19]; [e]Sque et al. [29]; [f]Hong and Chou [68].